Author(s): Sillanpää, Mika A. & Lehtinen, Teijo & Paila, Antti & Makhlin, Yuriy & Hakonen, Pertti

Title: Continuous-Time Monitoring of Landau-Zener Interference in a Cooper-Pair Box

Year: 2006

Version: Final published version

Please cite the original version:

Sillanpää, Mika A. & Lehtinen, Teijo & Paila, Antti & Makhlin, Yuriy & Hakonen, Pertti. 2006. Continuous-Time Monitoring of Landau-Zener Interference in a Cooper-Pair Box. Physical Review Letters. Volume 96, Issue 18. 187002/1-4. ISSN 0031-9007 (printed). DOI: 10.1103/physrevlett.96.187002.

Continuous-Time Monitoring of Landau-Zener Interference in a Cooper-Pair Box

Mika Sillanpää,[1] Teijo Lehtinen,[1] Antti Paila,[1] Yuriy Makhlin,[2,1] and Pertti Hakonen[1]
[1]Low Temperature Laboratory, Helsinki University of Technology, FIN-02015 HUT, Finland
[2]Landau Institute for Theoretical Physics, 119334 Moscow, Russia
(Received 9 December 2005; published 9 May 2006)

Landau-Zener (LZ) tunneling can occur with a certain probability when crossing energy levels of a quantum two-level system are swept across the minimum energy separation. Here we present experimental evidence of quantum interference effects in solid-state LZ tunneling. We used a Cooper-pair box qubit where the LZ tunneling occurs at the charge degeneracy. By employing a weak nondemolition monitoring, we observe interference between consecutive LZ-tunneling events; we find that the average level occupancies depend on the dynamical phase. The system's unusually strong linear response is explained by interband relaxation. Our interferometer can be used as a high-resolution Mach-Zehnder–type detector for phase and charge.

DOI: 10.1103/PhysRevLett.96.187002 PACS numbers: 74.50.+r, 73.23.Hk

The Landau-Zener (LZ) tunneling is a celebrated quantum-mechanical phenomenon, taking place at the intersection of two energy levels that repel each other [1]. The LZ theory, developed in the early 1930s in the context of slow atomic collisions [2–4] and spin dynamics [5], demonstrated that transitions are possible between two approaching levels as a control parameter is swept across the point of minimum energy splitting. The asymptotic probability of a LZ-tunneling transition is given by [2–5]

$$P_{\mathrm{LZ}} = \exp\left(-2\pi\frac{\Delta^2}{\hbar v}\right), \tag{1}$$

where $v \equiv d(\varepsilon_1 - \varepsilon_0)/dt$ denotes the variation rate of the energy spacing for noninteracting levels, and 2Δ is the minimum energy gap.

Yet for truly quantum-mechanical systems, more fundamental is the transition *amplitude*, which allows for interference. As two atoms collide, the wave-function phase accumulated between the incoming and outgoing traversals varies with, e.g., the collision energy giving rise to Stueckelberg oscillations in the populations [6]. Typically, however, the phase is large and rapidly varies with energy, which allows one to average over these fast oscillations [4,7], neglecting the interference.

Recently, quantum coherence in mesoscopic Josephson tunnel junctions has been investigated extensively [8–11]. In these artificial two-level systems, energy scales can easily be tuned into a range feasible for studies of fundamental phenomena. We used a charge qubit based on a Cooper-pair box (CPB) to obtain the first evidence of quantum interference associated with Landau-Zener tunneling in nonatomic systems. A continuous nondemolition measurement developed by us [12], which provides minimal backaction to the qubit, allowed for monitoring the average level occupancies of the CPB and thus observation of the LZ interference.

Our CPB is a single-Cooper-pair transistor (SCPT) embedded into a superconducting loop. The island has the charging energy $E_C = e^2/(2C) \sim 1$ K, and the junctions have the Josephson energies $E_J(1 \pm d)$, where d quantifies the asymmetry. The SCPT is equivalent to a CPB, but with a Josephson energy of $2E_J\cos(\phi/2)$ tunable by the superconducting phase across the two junctions, $\phi = 2\pi\Phi/\Phi_0$. When $E_C \gg E_J$, the Hamiltonian of the CPB is conveniently written in the eigenbasis $\{|2ne\rangle\}$ of the island charge operator, taking only two charge states into account:

$$H = -\frac{1}{2}B_z\sigma_z - \frac{1}{2}B_x\sigma_x = \begin{pmatrix} \epsilon(n_g) & -\Delta \\ -\Delta & -\epsilon(n_g) \end{pmatrix}, \tag{2}$$

where $\epsilon = -\frac{1}{2}B_z = -2E_C(1 - n_g)$ and $\Delta = \frac{1}{2}B_x = E_J\cos(\phi/2)$. The asymmetry $d \neq 0$ in Josephson energies would limit the minimum off-diagonal coupling $|\Delta|$. The eigenvalues of Eq. (2), $E_0(n_g, \phi)$ and $E_1(n_g, \phi)$, are the two lowest bands as illustrated by Fig. 1(a). By $|0\rangle = [1, 0]^{\mathrm{T}}$ and $|1\rangle = [0, 1]^{\mathrm{T}}$, we denote the corresponding (n_g, ϕ)-dependent eigenfunctions. Far from the crossing, they are roughly charge eigenstates.

The Hamiltonian of Eq. (2) is similar to the original LZ problem, and the linearly growing band gap $E_1 - E_0 \approx \varepsilon_1 - \varepsilon_0 = 4E_C(1 - n_g)$ has the minimum 2Δ at the charge degeneracy (avoided crossing) at $n_g = 1$. As n_g is swept through this point (similar to the interatomic distance during a collision), one obtains the asymptotic transition probability between levels 0 and 1 as in Eq. (1). This kind of incoherent limit of the LZ problem has also been observed in superconducting qubits [10].

More fundamentally, however, the asymptotic probability in Eq. (1) comes from the unitary transformation taking place at the avoided crossing [13,14]:

$$U_1 = \begin{pmatrix} \cos(\theta/2)\exp(i\tilde{\phi}_S) & i\sin(\theta/2) \\ i\sin(\theta/2) & \cos(\theta/2)\exp(-i\tilde{\phi}_S) \end{pmatrix}. \tag{3}$$

Here, $\sin^2(\theta/2) = P_{\mathrm{LZ}}$. The phase jump $\tilde{\phi}_S = \phi_S - \pi/2$ is due to the Stokes phase ϕ_S related to the general Stokes phenomenon [15]. It depends on the adiabaticity parameter $\delta = \Delta^2/\hbar v$ [cf. Eq. (1)], viz., $\phi_S = \pi/4 + \arg[\Gamma(1 - i\delta)] + \delta(\ln\delta - 1)$, where Γ is the Gamma function. In

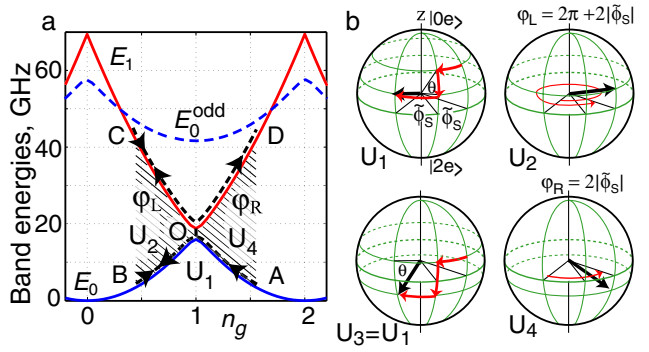

FIG. 1 (color online). Landau-Zener interference in a CPB. (a) The energy diagram: As n_g is modulated, the CPB evolves from the initial state A through the avoided crossing O ($n_g = 1$) towards B (no LZ tunneling) or C (with LZ tunneling). On the return journey, the final state D is reached by remaining on the excited band (from C) or by LZ tunneling (from B). The dynamical phases $\varphi_{L,R}$ are accumulated between O and the turning points. The uppermost dashed line represents the odd parity state $E_0^{\rm odd}$. (b) Interpretation of one cycle of LZ interference as four spin rotations on the Bloch sphere, with one possible set of $\varphi_{L,R}$ yielding constructive interference (see text). The black arrows indicate the final position of the Bloch vector after each step. Number states of the island charge $|2ne\rangle$ are aligned along the z axis.

the adiabatic limit $\phi_S \to 0$, and in the sudden limit $\phi_S = \pi/4$. On the Bloch sphere, a single LZ event [Eq. (3)] is seen as a combination of x and z rotations [U_1 and U_3 in Fig. 1(b)].

The natural manner to look for quantum coherence in LZ tunneling is to repeat the level crossing faster than the relevant time scales, as suggested by Shytov *et al.* [16]. Indeed, subsequent LZ-tunneling events with time interval τ_p can interfere, provided phase coherence is preserved and these events do not overlap [13,14], $\tau_z < \tau_p < \tau_{\rm coh}$. Here, the time of an LZ-tunneling event [17] is $\tau_z \sim \sqrt{\hbar/v}\max(1, \sqrt{\Delta^2/\hbar v})$. In charge qubits, it is easy to make $\tau_z \ll \tau_{\rm coh}$, where the coherence time is $\tau_{\rm coh} = \min(T_1, T_2)$ with T_1 and T_2 corresponding to the relaxation and dephasing time, respectively. For example, $\Delta = 2$ GHz and $v = 40$ GHz per 1 ns give $\tau_z \sim 0.1$ ns, which is well within experimental reach.

To generate the required conditions, we used a strong gate charge sweep $n_g(t) = n_{g0} + \delta n_{\rm rf}\sin(\omega_{\rm rf}t)$, in general offset from the crossing point. One cycle takes the CPB twice through the crossing and involves two dynamical phase shifts φ_L and φ_R, on the left and right sides:

$$\varphi = -\frac{1}{\hbar}\int [E_1(n_g(t)) - E_0(n_g(t))]dt. \qquad (4)$$

During a single drive cycle, the state vector evolves according to the transformation $U = U_4U_3U_2U_1$, which is illustrated in Fig. 1(b) as successive spin rotations (σ are the Pauli matrices, and $U_3 = U_1$):

$$U = \exp(-i\tfrac{1}{2}\varphi_R\sigma_z)U_1\exp(-i\tfrac{1}{2}\varphi_L\sigma_z)U_1. \qquad (5)$$

The transition amplitude $p_{\rm AD} = \langle\Psi|1\rangle = \langle 0|U^\dagger|1\rangle$ is the z projection of the Bloch vector. Evaluating Eq. (5) we find $p_{\rm AD} = i\exp(i\varphi_R/2)\cos(\varphi_L/2 - \tilde{\phi}_S)\sin(\theta)$, and the probability $P_{\rm AD} = |p_{\rm AD}|^2$ of reaching the point D:

$$|p_{\rm AD}|^2 = 2P_{\rm LZ}(1 - P_{\rm LZ})[1 + \cos(\varphi_{\rm L} - 2\tilde{\phi}_S)]. \qquad (6)$$

It is easy to see in Fig. 1(b) that $P_{\rm AD}$ is generally maximized (constructive interference) when the z rotations bring the Bloch vector back to the starting meridian, for then the total x rotation is maximized. This is achieved when the total phase $\varphi_L - 2\tilde{\phi}_S$ is a multiple of 2π. Under continuous driving, this has the obvious generalization which corresponds to the Bloch vector rotating stepwise around a fixed axis in the x-y plane; the condition

$$\varphi_{L,R} - 2\tilde{\phi}_S \text{ are multiples of } 2\pi \qquad (7)$$

ensures constructive interference (50% time-averaged populations of both levels). For example, in the adiabatic limit, $\varphi_{L,R}$ have to be odd multiples of π. The resonance conditions in Eq. (7) are seen overlaid in Fig. 3 (see below) as the black solid and dashed lines.

Our experimental scheme is illustrated in Fig. 2. The weak, continuous measurement signal tracks the time average, subject to a strong LZ drive, of the Josephson capacitance of a CPB: $C_{\rm eff} \propto \frac{\partial^2 E(\phi,n_g)}{\partial n_g^2}$, probed at $f_0 = 803$ MHz. The scheme is discussed in detail in Ref. [12]. The difference in $C_{\rm eff}$ for the levels 0, 1 allows us to determine the average state of the CPB (see the discussion below).

We made extensive scans of the CPB reflection by varying the LZ-drive frequency $f_{\rm rf} = 0.1$–20 GHz and its amplitude $\delta n_{\rm rf} = 0$–3 electrons, as well as the qubit bias n_{g0} and ϕ. We observe a clear interference pattern (Fig. 3) whose main features confirm the coherent LZ-tunneling picture: (1) onset of the interference speckles where the rf drive just reaches the avoided crossing, with

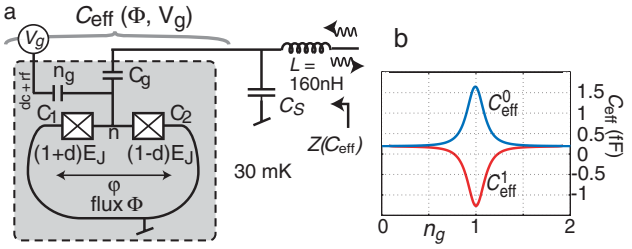

FIG. 2 (color online). Schematics of our experiment. (a) The resonant frequency $f_0 \sim 800$ MHz of the lumped-element LC circuit is tuned by the Josephson capacitance $C_{\rm eff}$ of the CPB shown in the scanning electron micrograph. The maximum CPB Josephson energy $2E_J = 12.5$ GHz could be tuned down to 2.7 GHz by magnetic flux Φ. The total junction capacitance amounts to $C_J = C_1 + C_2 \sim 0.44$ fF, yielding a Coulomb energy of $e^2/2(C_J + C_g) = 1.1$ K. (b) $C_{\rm eff}$ calculated for the two lowest levels of our CPB with $E_J/E_C = 0.27$ and asymmetry $d = 0.22$, at $\phi = 0$.

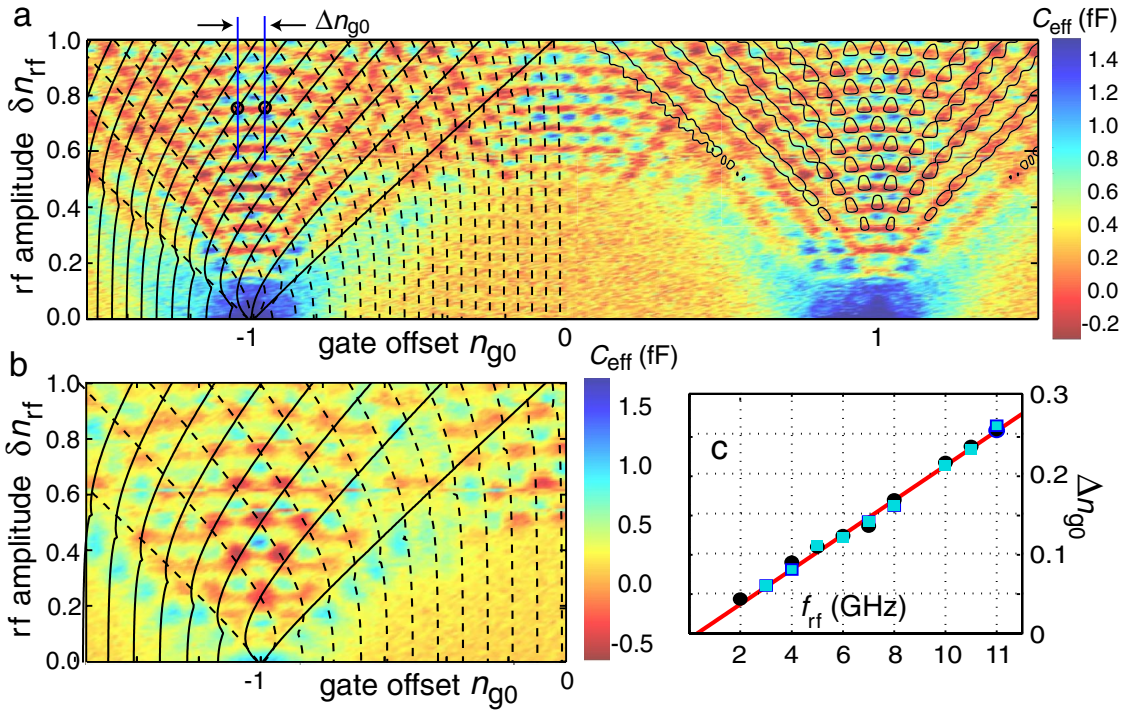

FIG. 3 (color online). Interference patterns, measured via the microwave phase shift. (a) $f_{\rm rf} = 4$ GHz and phase $\phi = 0$ (i.e., level repulsion $2\Delta = 2E_J = 12.5$ GHz). The color codes indicate the equivalent capacitance obtained using standard circuit formulas. Around $n_{g0} = -1$, the conditions of constructive Landau-Zener interference are illustrated: $\varphi_L - 2\tilde{\phi}_S$ (solid lines) and $\varphi_R - 2\tilde{\phi}_S$ (dashed line) are multiples of 2π [see Eq. (7)], with the v-dependent Stokes phase ϕ_S. The highest (red) population of the upper state is expected when both conditions are satisfied. The equicapacitance contour $C_{\rm eff} = 0$ around $n_g = 1$, obtained from the simulation of the Bloch equations (Fig. 4), agrees well with the predicted resonance grid and with the data. (b) The corresponding measurement with $f_{\rm rf} = 7$ GHz. (c) The average gate spacing between the central interference peaks [see (a)], for the phase bias 0 (square) and π (circle). The expected linear behavior yields a fit $E_C = 1.1$, about 25% higher than we obtained by rf spectroscopy [12].

a linear dependence between n_{g0} and the rf amplitude; (2) the density of the dots is proportional to $1/f_{\rm rf}$ in the direction of n_{g0} as well as $\delta n_{\rm rf}$; (3) the pattern loses its contrast below a certain drive frequency, here at $f_{\rm rf} \sim 2$ GHz, due to the loss of phase memory over a single LZ cycle. Note also the destructive interference dots at high drives, where the qubit remains basically on the lowest level, thus vindicating the "coherent destruction of tunneling" [18].

We attribute the slight asymmetries in the data with respect to $n_g = \pm 1$ to background charge drift caused by the strong rf drive. The theory grids in Figs. 3(a) and 3(b) were calculated by the v-dependent Stokes phase ϕ_S. However, since the Stokes phase amounts typically only to a 10%–20% shift of the grid, roughnesses in the data do not allow a clear verification of such a small effect.

The patterns are $2e$ periodic in n_{g0} at weak rf excitation. At stronger excitation on the order of $e/2$, an additional, shifted pattern makes the signal almost e periodic [Fig. 3(a)]. The origin of these odd sectors can be understood from the energy diagram in Fig. 1: When the rf drive brings the system past a crossing point of E_1 and $E_0^{\rm odd}$, it becomes energetically favorable to enter an odd particle-number state [19], resulting in a shift by e in the interference pattern.

According to Eq. (7), the phase difference $\varphi_- \equiv \varphi_L - \varphi_R \simeq 2\pi \frac{4E_C(n_{g0}-1)}{\hbar\omega_{\rm rf}}$ is a multiple of 2π at resonances, implying the location of the population peaks on the lines of fixed rf amplitude with spacings $\Delta n_{g0} = \hbar\omega_{\rm rf}/(2E_C)$. We observe the expected linear frequency dependence, as illustrated in Fig. 3(c).

The magnitude of the response in Fig. 3 forces one to study a complicated relation between the relevant time scales. $C_{\rm eff}(n_{g0})$ generally has contributions from how both the energies and populations depend on n_g. Furthermore, one has to time average over the strong LZ swing in $n_g(t)$. Therefore, we have

$$C_{\rm eff}(n_{g0}) \propto \left\langle \frac{d^2}{dn_g^2}[p_0(n_g)E_0(n_g) + p_1(n_g)E_1(n_g)] \right\rangle. \quad (8)$$

The dominant contribution is determined by the relative magnitude of the time scales of the LZ drive $1/f_{\rm rf}$, time of the measurement swing $1/f_0$, and the relaxation time T_1 (we suppose $f_{\rm rf} \gg f_0$). (a) Long relaxation time, $T_1 \gg 1/f_0$. During the measurement swing, populations do not relax into their quasiequilibrium values, $d^2/dn_g^2(p_{0,1}(n_g)) = 0$ and $C_{\rm eff}$ is small. (b) A short relaxation time, $T_1 \ll 1/f_0$. The populations follow $p_{0,1}(n_g)$ according to the instantaneous ac gate charge due to the

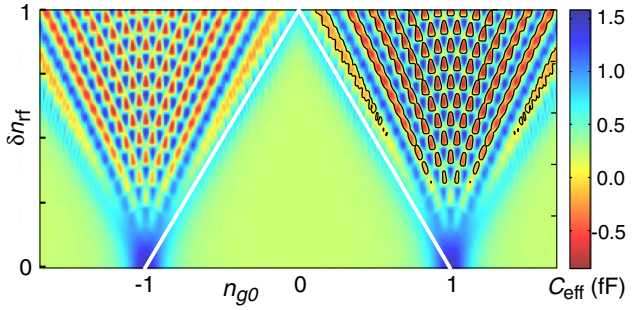

FIG. 4 (color online). Calculated $C_{\rm eff}$, using Bloch equations and linear-response theory, with $\alpha = 0.04$, $\delta n_{\rm ac} = 0.06e$ pp. The inclined white lines indicate the threshold of the LZ tunneling, where the driving signal $n_g(t)$ touches, but does not cross, a degeneracy point. The comparison with data in Fig. 3 is performed by the equicapacitance contours for $C_{\rm eff} = 0$ fF.

measurement swing, and Eq. (8) gives a large $C_{\rm eff}$. (c) Intermediate case. This corresponds to our experiment, where $T_1 \sim 5$ ns $\sim f_0 \sim 1$ ns. The value of $C_{\rm eff}$ is between (a) and (b). Therefore, we have a somewhat unexpected result that the magnitude of the measured response can be *increased* by relaxation.

To begin with, we numerically solved the Bloch equations [20,21]. We assumed that the T_1 and T_2 relaxation times are dominated by charge noise, modeled by an Ohmic bath with the strength $\alpha = (1 + [C_1 + C_2]/C_g)^{-2} \frac{2e^2}{h} R$, where R is the effective impedance of the gate voltage circuit. For our sample, $\alpha \sim 10^{-2}$ due to strong coupling to the environment via the gate. Various descriptions of dissipation are expected to yield the same result: one can show that in the description of crossing a narrow degeneracy region, dissipation can be effectively described by a few constants (cf. Ref. [16]).

In order to properly include the interplay between the time scales as described above, we used the linear-response theory to extract $C_{\rm eff}$, with a weak measurement ac signal on, of amplitude $\delta n_{\rm ac} = C_g \delta V_{\rm ac}$. We calculate the time-dependent expectation value for the charge Q_g on C_g, viz., $\langle Q_g \rangle(t) = {\rm Tr}(\rho * Q_g)$, where $Q_g = C_g(\delta V_{\rm ac} - dE/edn_g)$, and the density matrix is expressed in the energy eigenbasis. From $\langle Q_g \rangle(t)$ we pick up its quadrature components, $Q_{\omega_{\rm in}}$ and $Q_{\omega_{\rm out}}$, at the measurement frequency. The presence of the small resistive component $Q_{\omega_{\rm out}}$ is equivalent to having dissipation. By modeling the input impedance as $C_{\rm eff}$ in series with a small resistor, we find from the imaginary part $C_{\rm eff} = \frac{Q^2_{\omega_{\rm in}} + Q^2_{\omega_{\rm out}}}{Q_{\omega_{\rm in}} \delta V_{\rm ac}}$. The resulting capacitance at $f_{\rm rf} = 4$ GHz is illustrated in Fig. 4. The values $\alpha = 0.04$ and $\delta n_{\rm ac} = 0.03$ were taken in order to match the measured pattern. This corresponds at the degeneracy point to $T_2 \sim 0.5$ ns which is close to other estimates. The calculation is seen to reproduce the major features of the measured interferograms [22].

The LZ interference in Fig. 1(a) can also be interpreted as two partial waves, *AOBOD* and *AOCOD*, similarly to an optical Mach-Zehnder interferometer [23]. We propose to apply the LZ interferometry for sensitive detection of phase and charge [12,24–26], where it can be viewed as integrating phase amplifier for the superconductor phase ϕ across the device. The interferometer transforms tiny changes of ϕ (or magnetic flux Φ) into a huge modulation of the wave-function phase φ by basically integrating the hatched area [11] in Fig. 1, but with a limitation on the measurement signal amplitude.

Fruitful discussions with R. Fazio, M. Feigelman, T. Heikkilä, F. Hekking, M. Paalanen, and A. Shnirman are gratefully acknowledged. This work was financially supported by the Academy of Finland, the National Technology Agency, and the Vaisala Foundation of the Finnish Academy of Science and Letters.

[1] J. von Neumann and E. Wigner, Phys. Z. **30**, 467 (1929).
[2] L. Landau, Phys. Z. Sowjetunion **2**, 46 (1932).
[3] C. Zener, Proc. R. Soc. A **137**, 696 (1932).
[4] E. C. G. Stueckelberg, Helv. Phys. Acta **5**, 369 (1932).
[5] E. Majorana, Nuovo Cimento **9**, 43 (1932).
[6] D. Coey, D. C. Lorents, and F. T. Smith, Phys. Rev. **187**, 201 (1969).
[7] L. Landau, Phys. Z. Sowjetunion **1**, 88 (1932).
[8] Y. Nakamura, Yu. A. Pashkin, and J. S. Tsai, Nature (London) **398**, 786 (1999).
[9] Yu. Makhlin, G. Schön, and A. Shnirman, Rev. Mod. Phys. **73**, 357 (2001).
[10] A. Izmalkov *et al.*, Europhys. Lett. **65**, 844 (2004).
[11] L. Y. Gorelik *et al.*, Phys. Rev. Lett. **81**, 2538 (1998).
[12] M. A. Sillanpää *et al.*, Phys. Rev. Lett. **95**, 206806 (2005).
[13] E. Shimshoni and Y. Gefen, Ann. Phys. (N.Y.) **210**, 16 (1991).
[14] Y. Kayanuma, Phys. Rev. A **55**, R2495 (1997).
[15] M. V. Berry, in *Asymptotics Beyond All Orders*, edited by H. Segur and S. Tanveer (Plenum, New York, 1991), p. 1.
[16] A. V. Shytov, D. A. Ivanov, and M. V. Feigel'man, Eur. Phys. J. B **36**, 263 (2003).
[17] K. Mullen *et al.*, Phys. Rev. Lett. **62**, 2543 (1989).
[18] F. Grossmann *et al.*, Phys. Rev. Lett. **67**, 516 (1991).
[19] J. Aumentado *et al.*, Phys. Rev. Lett. **92**, 066802 (2004).
[20] F. Bloch, Phys. Rev. **70**, 460 (1946).
[21] Yu. Makhlin, G. Schön, and A. Shnirman, cond-mat/0309049.
[22] The "ridges" connecting the maxima parallel to the gate offset axis arise as secondary interference maxima where $\tan(\varphi_L/2 - 2\tilde{\phi}_S)\cos\theta + \tan(\varphi_R/2 - 2\tilde{\phi}_S) = 0$. To obtain the ridges in Bloch simulations, we have to put $T_2 \gg T_1$, due to definition of the relaxation times in the instantaneous eigenbasis of the driven system.
[23] After submission of the present manuscript, a related, independent work on flux qubits appeared: W. D. Oliver *et al.*, Science **310**, 1653 (2005).
[24] M. A. Sillanpää, L. Roschier, and P. Hakonen, Phys. Rev. Lett. **93**, 066805 (2004).
[25] L. Roschier, M. Sillanpää, and P. Hakonen, Phys. Rev. B **71**, 024530 (2005).
[26] M. Sillanpää *et al.*, cond-mat/0510559.